

Characterization of Transmural Myocardial Wall Motion in Mouse Using High Resolution MR Tagging

J. Zhong^{1,2}, W. Liu³, and X. Yu^{1,2}

¹Biomedical Engineering, Case Western Reserve University, Cleveland, OH, United States, ²Case Center for Imaging Research, Case Western Reserve University, Cleveland, OH, United States, ³Philips Research North America, Briarcliff Manor, NY, United States

Introduction

Genetically manipulated mouse models are playing an important role in the investigation of human cardiac diseases. The development of rapid, noninvasive methods for characterizing ventricular wall motion in these animals can provide new opportunities to elucidate the molecular mechanisms of myocardial dysfunction. MR tagging provides a unique opportunity to examine regional myocardial wall motion noninvasively, as well as more comprehensively and serially. Current tagging methods are limited by their low tagging resolution (>0.6 mm), which hampers the quantification of transmural wall strains in mouse heart. High-resolution tagging through combined SPAMM11 sequence with shifted tag grids has been demonstrated in humans (1). However, the doubled tagging resolution from two separate data sets presents additional challenge to the post-processing of tagging images. As a result, there has been limited application of this high-resolution tagging method.

In the current study, we developed a novel HARP-base myocardial strain analysis method, which allows fast strain calculation of the high-resolution tagging images. The utility of such method was demonstrated in mouse heart by quantifying the transmural difference of normal and principal strains.

Methods

MR Imaging 2-month-old C57/BL6 mice (n=7) were scanned on a Varian (Varian Associates, Palo Alto, CA) 4.7T scanner with a 2.5 cm surface coil. Tagged SA images were acquired with 1 mm slice thickness at midventricle. For each acquisition, two sets of tagging images (0.6 mm tagging resolution) were acquired, a SPAMM11 and a SPAMM1 $\bar{1}$, leading to a shift of the tag grid by half a tagging voxel between the two data sets (Figure 1). Such approach yielded a final tagging resolution of 0.3 mm. Subsequently, ECG-triggered, gradient-echo images were acquired with the following imaging parameters: TE, 3 ms; field of view, 4 cm \times 4 cm; matrix size, 256 \times 128. 15 frames were acquired per cardiac cycle.

Image Analysis HARP-based analysis method allows automatic tracing of tag lines and direct quantification of the Lagrangian strain in myocardium (2). For 1D tagging, the two sets of tagging images with shifted tagging voxels can be expressed as

$$\begin{cases} I_1(p) = I_o(p)(1 + c_1 \cos(g^T p)), \\ I_2(p) = I_o(p)(1 + d_1 \sin(g^T p)) \end{cases}$$

where p is the spatial variable, $I_o(p)$ is the image without tagging, c_1 and d_1 are coefficients determined by the flip angles, and g corresponds to the gradient related spatial frequency. Therefore, the combined high-resolution tagging images can be expressed as

$$I_H = I_1(p)I_2(p) = I_o^2(p)(1 + c_1 \cos(g^T p))(1 + d_1 \sin(g^T p)).$$

The expansion of the above equation yields a second-order harmonic peak, $0.5I_o^2(p)c_1d_1 \sin(2g^T p)$, that gives rise to the doubled tagging resolution. However, direct extraction of this harmonic peak from the combined high-resolution image suffers from severe interference from adjacent harmonic peaks (Figure 2A), leading to inaccurate tag tracing and strain calculation (Figure 2B&C). Alternatively, we propose to extract the two first-order harmonic peaks separately from the two images with low-resolution tagging (Figure 2D), i.e., $I_o(p)c_1 \cos(g^T p)$ and $I_o(p)d_1 \sin(g^T p)$. Multiplication of these two harmonic peaks yields the same second-order harmonic peak in high-resolution image. Such an approach is less subject to imaging noise, therefore, leads to more accurate tag tracing and strain calculation (Figure 2E&F).

Results

Figure 3 shows normal and principal strains at peak systole. Endocardial myocardium exhibited greater radial strain (E_{rr} , $P < 0.05$) compared with that in epicardium, suggesting more pronounced wall thickening at the endocardium. Circumferential shortening (E_{cc}) was more uniform. Both principal strains, E_1 and E_2 , were significantly larger at the endocardium ($P < 0.05$). The prime angle, the angle between the direction of maximal lengthening and radial direction was similar: $19.4 \pm 8.5^\circ$ at endocardium and $19.1 \pm 8.2^\circ$ at epicardium.

Conclusion

In the current study, we demonstrated a HARP-based automatic analysis method for fast strain calculation in high-resolution tagging images. The proposed method is more efficient and more accurate comparing with direct harmonic peak extraction from combined high-resolution images. The reported normal and principal strains (except E_{cc}) were significantly greater at the endocardium compared with those at the epicardium. Such pattern of transmural strain heterogeneity was similar to that in the human heart. The current study provides the potential for finer wall motion quantification that allows transmural characterization of regional cardiac functions in mouse heart.

References

1. Stuber M, Fischer SE, Scheidegger MB, Boesiger P. Toward High-Resolution Myocardial Tagging. *Magnetic Resonance in Medicine* 1999;41:639-643.
2. Liu W, Chen J, Ji S, Allen JS, Bayly PV, Wickline SA, Yu X. Harmonic Phase MR Tagging for Direct Quantification of Lagrangian Strain in Rat Hearts after Myocardial Infarction. *Magnetic Resonance in Medicine* 2004;52:1282-1290.

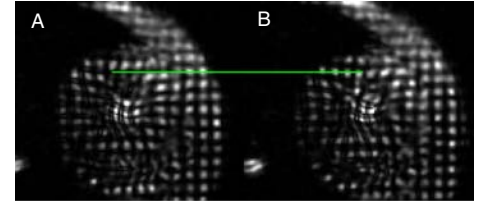


Figure 1. Two different tagging grids generated by SPAMM11 and SPAMM1 $\bar{1}$. A tag shift by half a tagging voxel can be seen at the green line between A and B.

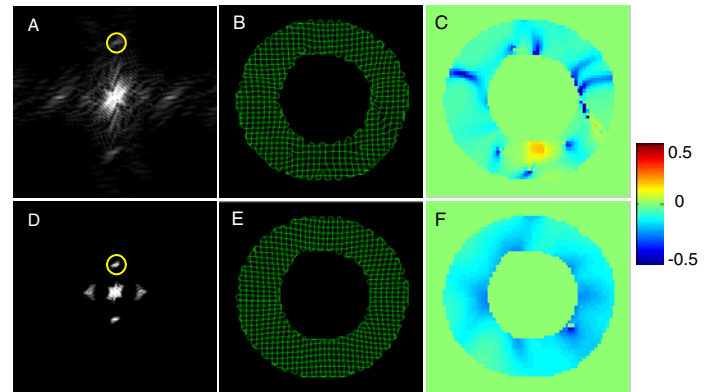


Figure 2. Fourier transform of combined high-resolution (A) and individual low-resolution (D) tagging images at peak systole. Yellow circles show the band-pass filter for harmonic peak extraction. Tag tracing and minimal principal strain maps from direct harmonic extraction (B,C) and our proposed method (E,F) at peak systole.

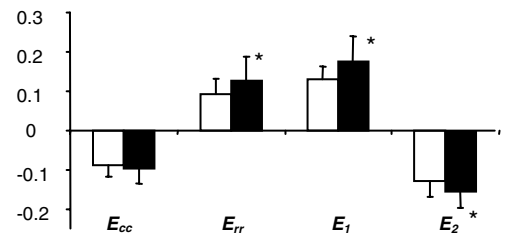


Figure 3. Average peak systolic normal and principal strains at endocardium (solid bars) and epicardium (open bars). E_{cc} : circumferential strain; E_{rr} : radial strain; E_1 : maximal principal strain; E_2 : minimal principal strain.